Heavy object handling by human-robot collaboration system with considering operability and positioning.

Kota. ABE [1], Yoshiyuki NODA[1]
1. University of Yamanashi, Kofu, Yamanashi, 400-8511, Japan
*Corresponding address: e-mail: g25dts01@yamanashi.ac.jp

Abstract: This paper concerns an object handling system using the human-robot collaboration technology. In the production sites of casting products, there are a lot of heavy object handling works such as core setting and disassembly of sand mold. It is required to apply the robotic automation to the heavy object handling. Especially for medium- to large-sized products, which are mainly produced in small lots of various types, it is challenging to adjust the robot motion to each kind of product, and work is still carried out by hand. Therefore, it is required to utilize a collaborative robot to assist the worker in the object handling. However, it is difficult to manipulate the robot directly at will. In this study, we propose the operational control system in the human-robot collaboration for the object handling work. In the proposed approach, we develop the admittance control system with the virtual model having Coulomb friction and viscous resistance for improving the operability and the positioning in the object handling. Furthermore, we also propose admittance control with Coulomb friction characteristics to enhance artificial reality. The efficacy of the proposed approach is verified by the experiments using the collaborative robot.

Keywords: admittance control; cooperative robot; direct manipulation; object handling;

1 Introduction

There are a lot of heavy handling works such as core setting and disassembly of sand mold in the production sites of casting products. Moreover, as production methods are shifting from mass production to high-mix low-volume production, factory automation is evolving from simple repetitive tasks to assembly tasks requiring non-routine and skillful operations, becoming more complex [1]. In addition, industrial robots, which are general-purpose machines, are being used to robotize production processes, but teaching robot motion requires specialized knowledge in coordinate input and motion programming. In recent years, to solve these problems, cooperative robots that can teach robot motion easily, such as direct teaching, are required [2-3].

As shown in Fig. 1, one possible application of cooperative robots is the collaborative assembly of heavy parts by a worker and a robot. The worker can directly manipulate the heavy parts while the cooperative robot grasps the object to reduce the workload. A force sensor is installed on the robot's hand to manipulate the robot directly, and the robot moves according to the manipulation force detected by the admittance control. This kind of human performance improvement using cooperative robots is becoming common [4]. However, it is difficult to say that the mass-damper system with virtual mass and viscous resistance can be applied to the virtual model of admittance control used in the cooperative human-robot system, because it does not provide good operability.

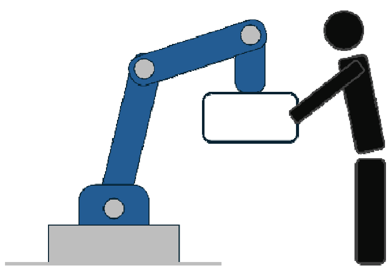

Fig. 1 Human-robot collaboration system

Therefore, in this study, we propose an admittance control method that considers both operability and position ability in the cooperative work between a human and a robot to transfer heavy objects. In the proposed method, a mass-damper system that combines viscous resistance and Coulomb friction is constructed as a virtual model of admittance control. Frequency analysis reveals that the proposed virtual model improves the operability. Furthermore, Coulomb friction is applied to the virtual model to create a feeling of operation close to reality.

Cooperative operation experiments with robots confirm the effectiveness of the proposed method.

2 Admittance control

Admittance control is a control model widely known as a technique to enable compliant behavior of robots [5]. Fig. 2 shows the block diagram of admittance control that allows direct manipulation. In admittance control, a force sensor placed at the robot's hand end detects the manipulation force applied to the grasping tool or the object attached to the robot's hand end. The detected manipulation force is given to the virtual model. Based on the virtual model, the robot motion is calculated, and the velocity command of the robot tip is output. The velocity commands are given to the robot controller, and the robot moves according to them. This study's virtual model consists of a mass damper system and a dead zone against the manipulation force. The dead zone is set so the robot does not move due to the force sensor's noise. The following equation (1) shows the manipulative force F_d through the dead zone for the manipulative force F detected by the force sensor.

$$F_d(t) = \begin{cases} 0, (|F(t)| \leq d) \\ \mathrm{sgn}(F(t))(F(t) - d, (|F(t)| > d) \end{cases} \quad (1)$$

Where d denotes the boundary value of the dead zone and t denotes time. This dead zone is considered to have similar characteristics to static friction. The operating force F_d is applied to the mass damper system through the dead zone.

The general mass-damper system is expressed as follows.

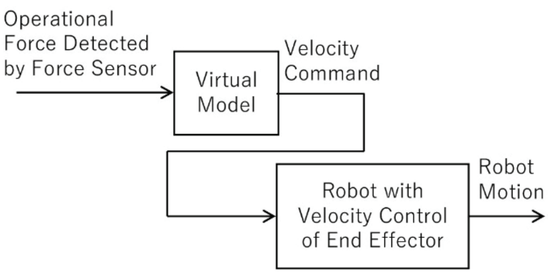

Fig. 2 Block diagram of admittance control in robot motion control system

$$m\dot{v}(t) + cv(t) = F_d(t) \quad (2)$$

Where m is the virtual mass, v is the velocity of the massive object, and c is the virtual viscosity coefficient.

2.1 Admittance control with damper characteristics combining viscous resistance and Coulomb friction

In most previous studies, as shown in equation (2), mass damper models with linear characteristics have been used as virtual models. In this study, we consider that frictional resistance is more dominant than viscous resistance in damping motion and propose a damping characteristic that combines viscous resistance and Coulomb friction. In the proposed method, the viscous resistance is assumed to be the characteristic of smooth motion from the stationary state to the start of motion. However, since the viscous resistance increases proportionally to the velocity, the system's operability deteriorates at high-speed motion. Therefore, after reaching a predetermined speed, the resistance value becomes the characteristic of Coulomb friction, eliminating the resistance value's speed dependence and improving operability at high speeds. In addition, we propose a virtual model with Coulomb friction characteristics even in the low-speed state of damping to improve positioning performance during damping. The virtual model of the mass-damper system proposed in this study is shown in the following equation.

$$\begin{cases} m\dot{v}(t) + cv(t) = F_d(t), (|v| \leq v_s \wedge t < t_1) \\ m\dot{v}(t) + \mathrm{sgn}(v)cv_s(t) = F_d(t), (|v| > v_s \vee t \geq t_1) \end{cases} \quad (3)$$

Where v_s denotes the boundary velocity in bounded viscous resistance. The viscosity coefficient c_s when the boundary velocity is exceeded is given by

$$c_s(t) = \frac{\mathrm{sgn}(v)cv_s}{v} = \frac{cv_s}{|v|} \quad (4)$$

Substituting equation (4) into equation (3), we obtain

$$\begin{cases} m\dot{v}(t) + cv(t) = F_d(t), (|v| \leq v_s \wedge t < t_1) \\ m\dot{v}(t) + c_s(v)v = F_d(t), (|v| > v_s \vee t \geq t_1) \end{cases} \quad (5)$$

The control is switched depending on the velocity value, as expressed by equation (5). This allows us to consider that when viscous resistance exceeds the boundary speed, the mass damper system's viscosity coefficient varies depending on the speed. The t_1 denotes the time of the first switch from viscous resistance to Coulomb friction. In the present study, the system operates smoothly from the stationary state according to the time condition using t_1 to achieve both operability and position ability.

If the viscosity coefficient varies with the steady-state speed, the transfer function is given by

$$\frac{V(s)}{F_d(s)} = \left.\frac{\frac{1}{m}}{s+\frac{c_e}{m}}\right|_{c_e=\begin{cases} c,(|v|\le v_s) \\ c_s(v),(|v|>v_s)\end{cases}} \quad (6)$$

$$= \left.\frac{\frac{1}{m}}{s+\frac{c_e}{m}}\right|_{c_e=\begin{cases} c,(|v|\le v_s) \\ c_s(v),(|v|>v_s)\end{cases}} \quad (7)$$

where ω_c is the breakpoint angular frequency and k is the gain.

The frequency response analyzes the switching from low speed to high speed in the proposed mass damper system with bound viscous resistance. The following equation from equation (7) gives the gain characteristics.

$$\left|\frac{V(\omega)}{F_d(\omega)}\right| = k\left.\sqrt{\frac{\left(\frac{\omega_c}{\omega}\right)^2}{1+\left(\frac{\omega_c}{\omega}\right)^2}}\right|_{c_e=\begin{cases} c,(|v|\le v_s) \\ c_s(v),(|v|>v_s)\end{cases}} \quad (8)$$

Therefore, the gain and the breakpoint angular frequency are expressed as follows.

$$k = \frac{1}{c_e} = \begin{cases} \frac{1}{c},(|v|\le v_s) \\ \frac{|v|}{cv_s},(|v|>v_s)\end{cases} \quad (9)$$

$$\omega_c = \frac{c_e}{m} = \begin{cases} \frac{1}{c},(|v|\le v_s) \\ \frac{|v|}{cv_s},(|v|>v_s)\end{cases} \quad (10)$$

The gain characteristics of equation (8) and the breakpoint frequency of equation (10) are graphed in Fig. 3. In Fig. 3, the virtual mass is set to $m = 10$[kg], the virtual viscosity coefficient is set to c =60[kg/s], and the boundary velocity is set to $v_s = 7$[m/s]. The range of velocity v is set to $1 \le v \le 30$. The mesh surface plot shows the frequency response varying with each steady-state velocity, and the red line indicates the breakpoint angular frequency. The red line indicates the breakpoint angular frequency. The results show that beyond the boundary velocity, the gain increases and the breakpoint frequency decreases as the steady-state velocity increases.

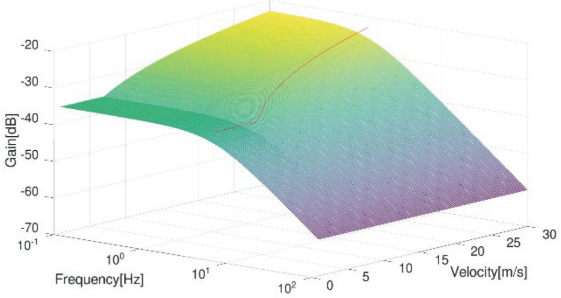

Fig. 3 Frequency response and cut-off frequency varying by velocity

Also, substituting equations (8), (9), and (10), we obtain

$$\left|\frac{V(\omega)}{F_d(\omega)}\right| = \left.\sqrt{\frac{1}{m^2\omega^2+c_e^2}}\right|_{c_e=\begin{cases} c,(|v|\le v_s) \\ c_s(v),(|v|>v_s)\end{cases}} \quad (11)$$

where $m^2\omega^2 \gg c_e^2$ can be approximated by

$$\left|\frac{V(\omega)}{F_d(\omega)}\right| = \left.\sqrt{\frac{1}{m^2\omega^2+c_e^2}}\right|_{c_e=\begin{cases} c,(|v|\le v_s) \\ c_s(v),(|v|>v_s)\end{cases}} \quad (12)$$

This means the gain characteristics are independent of the viscosity coefficient at high frequency up to the breakpoint frequency. Therefore, beyond the boundary velocity, the gain in the low frequency band increases with the increase of the steady-state velocity. In contrast, the gain characteristics in the high-frequency band remain unchanged.

The results of this analysis suggest that in admittance control equipped with a mass-damper system that combines viscous resistance and Coulomb friction, a small force can increase the velocity in the region beyond the boundary velocity, improving the operability.

2.2 Coulomb friction model

Another way to achieve operability and position ability is to introduce admittance control with only Coulomb friction, the same as the real environment. In this study, we propose an admittance control with Coulomb friction. The proposed method sets the model parameters of Coulomb friction so that the user can efficiently operate the system [5]. This allows us to evaluate the effect of friction on operability.

This study uses a virtual model of the wiping training system [5] used in upper limb rehabilitation. The virtual model of Coulomb friction is shown in the following equation.

$$m_v\dot{v}_{vi}(t) = \begin{cases} -c_v v_{vi}(t), (F_o^2 \le \mu_s^2 \text{ and } v_v^2 \le v_{vst}^2) \\ -c_v v_{vi}(t) - \mu_k u_i + F_i(t), (\text{else}) \end{cases}$$

(13)

Here, the

$$F_o^2 = F_x^2 + F_y^2 \quad (14)$$

$$v_v^2 = v_x^2 + v_y^2 \quad (15)$$

$$u_i = \begin{cases} \mathrm{sgn}(v_{vi}), (v_{vi}^2 \geq v_v^2) \\ v_{vi}/v_v, (\mathrm{else}) \end{cases} \quad (16)$$

The upper part of equation (13) denotes the stationary state, and the lower part of equation (13) represents the motion state. Also, m_v is the virtual mass, c_v is the virtual viscous damping coefficient, and v_{vi} is the velocity of each axis of the robot tool on the virtual model. And F_o denotes the magnitude of the combined x- and y-axis manipulation forces, and μ_s denotes the maximum static friction force. v_v denotes the absolute value of the robot tool velocity on the virtual model, and v_{vst} is the region where the robot tool is stationary, given as $v_{vst} \ll 1$. μ_k denotes the dynamic friction force, and u_i is the partial velocity of each axis when the magnitude of the robot tool velocity on the virtual model is normalized to 1, so that $u_x^2 + u_y^2$=1. Equation (16) is provided to prevent the dynamic friction force from being excessive due to noise from the force sensors or calculation errors in the controller.

Implementing equation (13) as a virtual model in admittance control introduces Coulomb friction in planar motion.

3 Subject experiment

In this experiment, the conventional linear mass damper model, the proposed fusion model of viscous resistance and Coulomb friction, and the Coulomb friction model are implemented in admittance control, respectively, and comparative experiments are conducted.

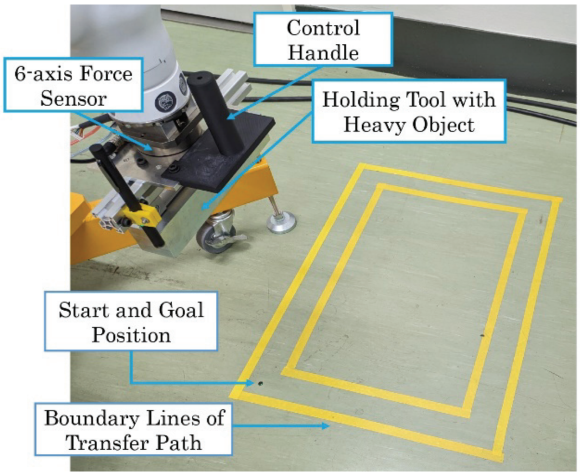

Fig. 4 Experimental apparatus with collaborative robot

Fig. 4 shows the heavy load transfer environment by cooperative work with a robot. The parameters of the conventional linear mass damper model and the proposed fusion model used in this experiment are virtual mass m = 8[kg], virtual viscosity c = 60[kg/s], boundary value of dead zone d = 3[N], and boundary velocity v_s = 0.07[m/s]. The parameters of the friction model are virtual mass m_v = 8[kg], virtual viscous damping coefficient c_v = 40.0, maximum static friction force μ_s = 0.0001, and dynamic friction force μ_k = 3.0.

The experiment will be conducted with four subjects, and the linear mass damper, fusion, and friction models will be trained and tested in this order. The first step of the experimental procedure is to train the subjects to become accustomed to the robot's operation. The training continues for an unlimited time until the subject feels comfortable. Subjects are also advised on how to apply force to manipulate the robotic arm. The subject can see the transfer path by the light emitted by the laser module attached to the robot tool on the floor. After the training, a test of robot operation is conducted. In the test, the subject performs 5 times one round of the path indicated by the yellow line as shown in Fig. 4. In the test, the robot is instructed to be conscious of passing through the center of the path. The conventional method, the proposed method, and the friction model conduct these training and testing processes.

Finally, a questionnaire based on the Likert scale is administered, and a comparison is made by subjective evaluation. The questionnaire will focus on lightness during operation, positioning, and operability, and the following eight items will be evaluated on a 5-point scale.

Q1. Did you feel the operation was light?
Q2. Did you find it easy to position?
Q3. Did you find it easy to operate?
Q4. Did you feel you could operate for long periods?
Q5. Did you find the controls familiar?
Q6. Did you feel you could maneuver faster?
Q7. Did you find the task easy to accomplish?
Q8. Did you find it easy to operate as per the operation path?

Items Q1, Q4, and Q6 are intended for lightness in operation, while items Q2 and Q8 evaluate positioning performance, and items Q3, Q5, and Q7 evaluate operability. For each question, five is "very applicable" and one is "not applicable at all.

3.1 Experimental results

The experimental results of this experiment are evaluated from the force and trajectory data for lightness in operation, maneuverability, and positioning, respectively.

3.1.1 Evaluation of lightness (derivation of integral value of force data)

The first step is to evaluate the lightness. This evaluation is made by taking the integral value of the force data and comparing the total amount of force input, considering the time of the entire operation. This is calculated for each subject and each test, and compared as a box-and-whisker diagram in Fig. 5. Here, each graph of the experimental results shows the results for the four subjects A to D. The vertical axis represents the integral of the force data, and the horizontal axis represents the linear mass damper model (1), the fusion model (2), and the friction model (3).

From Fig. 5, the force product of the operating force in the linear mass damper model was about 125[Ns], in the fusion model about 100[Ns], and in the Coulomb friction model 150 ~ 200[Ns]. As a result, the fusion model is the lightest for all subjects, and the friction model is the heaviest for all subjects.

This result shows that the fusion model is superior in lightness in the experimental results. On the other hand, the friction model is evaluated as the heaviest.

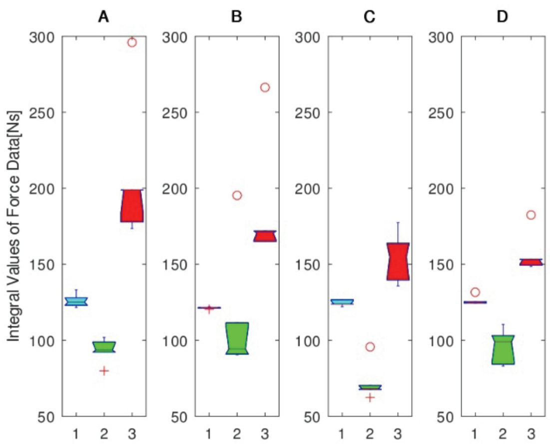

Fig. 5 Comparison of integral values of force data

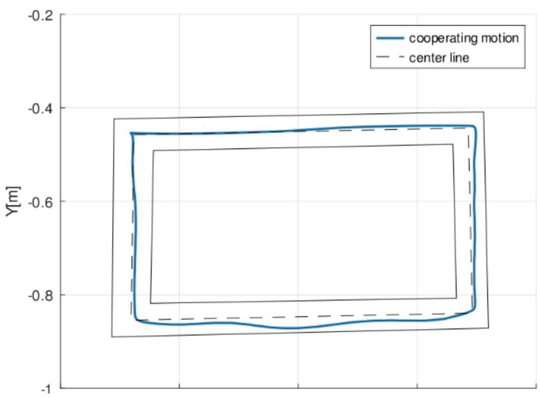

Fig. 6 Experimental results of cooperating motion

3.1.2 Evaluation of position ability (differential evaluation of goal position)

Next, we evaluate the positioning performance. In assessing the positioning performance, since the start and final stop positions are the same as shown in Fig. 6, the comparison is made based on the difference between them. A box-and-whisker diagram of the four subjects and their five results is demonstrated in Fig. 7.

The average stop is approximately 2 ~ 4[mm] in all the results. This result indicates that the Coulomb friction tends to be slightly lower regarding position ability. Still, the markers' 8[mm] diameter indicating the start and end positions suggests that the results suit all the methods.

3.1.3 Evaluation of operability (evaluation of trajectory data wobble)

The trajectory data evaluates the operability, as in the positioning assessment. In this experimental test, the subject is instructed to follow the light from the laser module along the center of the yellow frame, which indicates the transport path region of Fig. 4. Therefore, the operability is evaluated by the integral squared error concerning the center trajectory of the transport path region. The results are compared as box plots in Fig. 8.

The box-and-whisker plots show that the friction model is equivalent to or superior to the linear mass damper method except for subject A. The friction model is superior to the linear mass damper method except for subject B, which is superior to the linear mass damper method. Similarly, the fusion model has the worst results except for subject A.

We consider that the fusion model's experimental operability results are worse than those for the linear

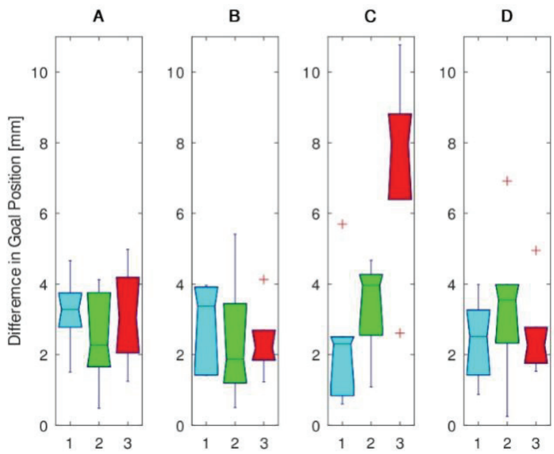

Fig. 7 Comparison of difference in goal position

mass damper because of the increased difficulty of operation due to the different behavior at the start and stop of the fusion model.

In the friction model, we believe that the Coulomb friction characteristics, which allow the model to behave in real space, are mainly responsible for the superior operability of the experimental results compared to the conventional linear mass damper method.

3.2 Subjective evaluation results

Fig. 9 shows the results of the questionnaire comparing the linear mass damper, fusion, and friction models. The questionnaire results show that items Q1 and Q6 show the superiority of the fusion model, and items Q2, Q3, Q4, Q7, and Q8 show the superiority of the friction model.

First, we check the evaluation of Q1, Q4, and Q6. Q1's lightness of operation and Q6's speed of operation confirm the fusion model's apparent superiority. On the other hand, the fusion model with light operability is not found to have an advantage regarding the possibility of long-term operation of Q4. This is due to the increase in the degree of difficulty of the operation. All lightness evaluations for the friction model are superior to those for the linear mass damper model. This contradicts the experimental results, which confirmed the heaviest weight. The velocity outputs of the linear mass damper and friction models are comparable to the friction model's results. This result suggests that the subject's perception of the control's weight varies depending on the velocity output of the operating force.

Next, we compare the positionality of Q2 and Q8.

The results show that the Coulomb friction model is superior in both cases. In addition, the friction model is superior in Q3 and Q7, which are related to evaluating

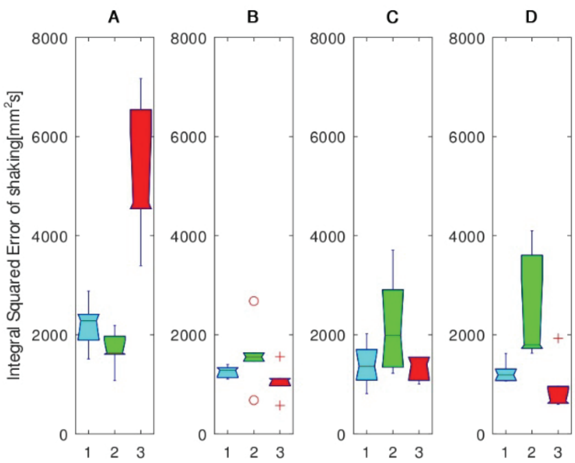

Fig. 8 Comparison of fluctuation on cooperating motion

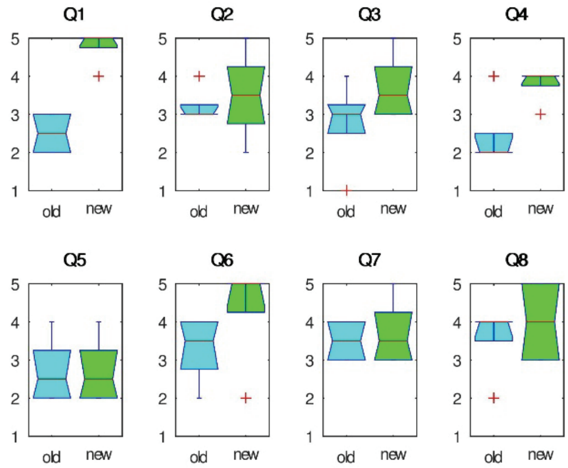

Fig. 9 Results of questionnaire by Likert scale

operability. The results for the operability items are consistent with the experimental results.

It can be concluded that the Coulomb friction model can perform the same actions as in real space, which is why such subjective evaluations exist.

4 Conclusions

This study proposes the operational control system using the admittance control method for the object handling by human-robot collaboration that considers operability. In the proposed admittance control, the mass-damper system with combining viscous resistance and Coulomb friction is implemented as the virtual model. The frequency analysis shows that the proposed virtual model improves the operability.

In this study, we also proposed the model using Coulomb friction for the virtual model's damping characteristics. We compared and verified which of the three models, the conventional linear model, the proposed fusion model of viscous resistance and Coulomb friction, and the Coulomb friction model, human beings feel the most comfortable feeling of these three models through experiments using a cooperative robot to transfer heavy objects by direct manipulation of the robot.

As a result, we confirmed the validity of the proposed fusion model of viscous resistance and Coulomb friction in the item of lightness. However, the operation became more difficult due to the difference in behavior at the start and end of the operation. Compared to the three models, the Coulomb friction model was evaluated to have the best operability in the subject experiment.

From these results, we believe that the proposed fusion model of viscous resistance and Coulomb friction is suitable for operations that require a wide range of motions or repetitive operations over a long period. The Coulomb friction model is ideal for detailed operations due to its operability.

References

[1] N. Yamanobe, Y. Maeda, T. Arai, J. Watanabe, T. Kato, T. Sato, and T. Hatanaka, [Force Control Parameter Design Considering Cycle Time], Saikuru taimu o kōryo shita chikara seigyo paramēta sekkei (in Japanese), Journal of the Robotics Society of Japan, vol. 24, no. 4, 2006, pp.554-562.

[2] T. Sato, [Cooperative robots (cobots) pioneer innovation in production and living], Kyōdō robotto (kobotto) ga hiraku seisan to seikatsu no kakushin(in Japanese), lateral trunk, vol. 9, no. 2, 2015, p. 79-85.

[3] K. Harada and W. Wan, [On next-generation technologies for industrial robots], Sangyōyōrobotto no jisedai gijutsu ni tsuite.(in Japanese), Journal of the Robotics Society of Japan, vol. 37, no. 10, 2019, p. 915-918.

[4] Campeau-Lecours A, Otis MJ-D, Gosselin C. Modeling of physical human robot interaction: Admittance controllers applied to intelligent assist devices with large payload. International Journal of Advanced Robotic Systems. 2016;13(5).

[5] F. Dimeas and N. Aspragathos, "Reinforcement learning of variable admittance control for human-robot co-manipulation," 2015 IEEE/RSJ International Conference on Intelligent Robots and Systems (IROS), Hamburg, Germany, 2015, pp. 1011-1016.

[6] Y. Noda, [Development of Wiping Expertise System with Enhancing Realistic Sensation and Adjustable Exercise Load Using Force Display Technology], Rikikakutei zigizyutu wo motiita kōrinzyōkan to kunrenhuka no tyōsei wo kanō ni suru waipingukunrensisutemu no kaihatu (in Japanese), SI2018, 2018, p. 1818-1822.